Feasibility of CEST imaging on the guinea pig stifle at 9.4 T

M. Fenty[1], V. Kassey[1], F. Kogan[1], and R. Reddy[1]

[1]CMROI, Radiology, University of Pennsylvania, Philadelphia, PA, United States

Introduction: Osteoarthritis (OA) is a common and painful condition with a multi-factorial etiology of the musculoskeletal system affecting more than 50% of the U.S. population over 65 (1) (2). Degeneration of the articular cartilage tissue, which is believed to be a primary factor in the development of OA, is a slow process and typically takes decades to have full thickness loss, but can be significantly accelerated due to trauma or surgical procedures (3). Dunkin-Hartley guinea pigs have been shown to develop OA with the earliest stage of detection manifesting as early as three to four months of age. Therefore, the Dunkin-Hartley guinea pig model provides a practical system for the longitudinal studies of the progression of OA (3) (4) (5). Quantitative assessment of glycosaminoglycan (GAG) molecules can assist with assessment and treatment of cartilage degradation.

Chemical exchange between labile protein protons and bulk water can make MRI sensitive to information about the concentrations and environments of endogenous proteins (6). Chemical Exchange Saturation Transfer (CEST), a technique which uses the attenuation of bulk water magnetization through magnetization exchange with saturated labile protons, has become a popular method for measurement of metabolites with exchangeable protons. GAG contains amino groups ($-NH_2$) and hydroxyl groups (–OH) that exchange protons with bulk water that can be that exploited for CEST. This offers a potential endogenous marker for the determination of GAG content in tissue (7) (8). Hence, CEST may provide a sensitive and specific marker for GAG assessment. Here we will show preliminary results of implementation and optimization of CEST imaging using GAG-dependent contrast on healthy guinea pig cartilage samples on a 9.4 T Varian scanner.

Methods: Duncan-Hartley guinea pigs were obtained and maintained under an IACUC approved protocol. The left hind stifle joint was imaged using a CEST-prepared GRE sequence on a 9.4 Tesla Varian horizontal 20 cm bore scanner. One three-month old guinea pig stifle was surgically removed. Muscle and adipose tissue was surgically removed and the femur was submerged in nearly room-temperature 1% agarose solution to eliminate motion. A custom 3 cm long solenoid coil was used for imaging. *CEST optimization:* We implemented a series of pre-saturation pulses with various amplitudes and durations appended to a stock 2D GRE readout. CEST-B_{1amp}: 25, 50, 75, 125 Hz, CEST-$B_{1duration}$ = 1, 2 sec. A train of 6 square pulses was implemented for the CEST saturation pulse. For 8 iterations used, whole z-spectra were acquired in step sizes of 0.1 PPM ranging from 4 ppm -> -4 ppm. *B_0 optimization*: Performed through localized STEAM voxel shimming over the joint cartilage and through post-processing correction from z-spectra. *B_1 optimization:* Performed using a "flip-crush" procedure. A series of rapid image acquisition was performed while titrating a hard-pulse amplitude until a signal minimum (flip = 90º) was achieved along a band within the center of the joint. This pulse calibration was used for all subsequent imaging. GRE readout had the following parameters: TE = 5.15 ms, TR = 11.8 ms, matrix = 256 x 256, resolution = 0.97 mm^2 x 0.75 mm, α = 20º. A four-short segmented centric acquisition was used to mitigate loss of CEST-contrast while approaching the steady state. A delay of 4 seconds was appended to the end of each segment to allow full recovery of longitudinal magnetization between CEST-preparatory segments. A series of far off-resonant images were also collected for the 8 iterations mentioned above: 50, 20, 10, 5, -5, -10, -20, -50 ppm which are used to determine apparent CEST effect of the cartilage.
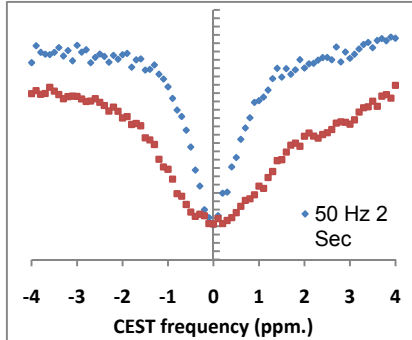
Results:

Figure 1: Optimization of both saturation power and duration has demonstrated that a CEST duration of 2 second and either 50 or 125 Hz generates the greatest CEST effect in the 3 month old tissue sample. In the 50 Hz case, two noticeable CEST peaks exist downfield of bulk water while there are three in the 125 Hz case. These dips are indicative of exchangeable protons

PPM	50 PPM		Neg. PPM	
	50 Hz	125 Hz	50 Hz	125 Hz
0.9-1.1	4.51%	1.56%	9.01%	7.77%
2.3-2.5	0.22%	8.83%	0.97%	18.80%
2.6-3	2.59%	8.45%	5.58%	17.70%

Table 1: Apparent CEST effect for the two optimized duration / power combinations is shown. Two methods to calculate CEST effect are shown: dividing by far off-resonance (50 ppm) and dividing by negative off-resonance. Results show strong CEST effect for several frequencies.

There is a large CEST effect in the ~1 PPM range for the 50 Hz peak (indicative of protons from –OH). In the 125 Hz spectra, there is a large CEST effect between 2.3-3 ppm indicative of –NH protons.

There is a large change in apparent CEST effect depending on which method to report is used (average increase ~300%).
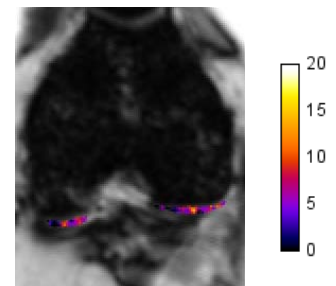

Figure 2: Representative CEST map of the three month old femoral condyle utilizing a 3 ppm saturation pulse for 2 seconds at 125 Hz. CEST effect was normalized with the 50 ppm. Color-bar is in percentage CEST effect.

Conclusions: The preliminary results presented here indicate the potential use for endogenous CEST contrast to be exploited to quantify relative content of labile –NH and –OH protons present in glycosaminoglycan chains of guinea pig stifles. Two methods widely used to calculate apparent CEST effect demonstrate large and significant variations in values. Studies are ongoing to transfer optimization protocol to in vivo guinea pig use to quantify cartilage degradation as a result of OA.

References: **1.** Felson D., et. al., Arthritis Rheum 1995;38(10):1500-1505. **2.** Seibel MJ., et. a. San Diego: Academic Press; 1999. xx, 672 p. p. **3.** Moskowitz RW., et. al., Philadelphia: Saunders; 2001. xx, 674 p., 676 p. of plates p. **4.** McDougall J., et. al., Pain 2009;141(3):222-232., **5.** Tessier J., et. al., Osteoarthritis Cartilage 2003;11(12):845-853. **6.** Wolff et. al., J. Magn. Reson. 86,, 164-169. **7.** Ward KM., et. al., *J. Magn. Reson.* 143, 79-87. **8.** Zhou J., et. al., *Prog. NMR Spectr.* 48, 109-136